

# Quantum error correction via multi-particle discrete-time quantum walk

Ryo Asaka<sup>1,\*</sup> and Ryusei Minamikawa<sup>1,†</sup>

<sup>1</sup>*Department of Physics, Tokyo University of Science,  
Kagurazaka 1-3, Shinjuku-ku, Tokyo 162-8601, Japan*

We propose a scheme of quantum error correction that employs a multi-particle quantum walk defined on nested squares, each hosting a single particle. In this model, each particle moves within its own distinct square through iterations of three discrete-time steps. First, a particle updates its two-level internal *coin* state. Next, it either moves to an adjacent vertex or stays put, depending on the outcome. Finally, it interacts with another particle if these particles arrive at the nearest-neighbor vertices of the two adjacent squares, acquiring a phase factor of  $-1$ . Because a single particle represents a three-qubit state through its position and coin state, Shor's nine-qubit code is implemented using only three particles, with two additional particles for syndrome measurement. Furthermore, by exploiting gauge symmetry, our scheme achieves redundant encoding, error correction, and arbitrary operations on the encoded information using only nearest-neighbor interactions.

*Introduction*— The discrete-time quantum walk, a quantum counterpart to the classical random walk, is a mathematical model of a particle that evolves in discrete-time steps via two unitary operators, coin-flipping and position-shifting [1, 2]. In each step, the coin-flipping operator changes the *coin* state of the particle, which is spanned by  $|0\rangle_c$  and  $|1\rangle_c \in \mathbb{C}^2$ . The subsequent position-shifting operator moves the particle to another position based on the outcome of the coin-flipping. Since the coin state may form a quantum superposition of both  $|0\rangle_c$  and  $|1\rangle_c$ , the particle simultaneously moves in different directions and becomes widely distributed across space as a quantum superposition.

Thanks to its unique quantum spatial distribution, the discrete-time quantum walk plays a crucial role in several quantum algorithms. Representative examples are quantum walk-based search algorithms in computational space, structured as hypercubes [3–5], multi-dimensional lattices [6, 7], bipartite graphs [8–10], or more complicated graphs [11–13]. They provide a quadratic speed-up over classical counterparts when searching for the target data in the computational space.

Implementations of quantum computation are also important applications of the discrete-time quantum walk. One example is a universal quantum computer based on a single-particle discrete-time quantum walk [14]. The architecture consists of many wires and graphs through which a flying qubit propagates in discrete time steps. Another example is an application to quantum random access memory [15]. In discrete-time steps, the register spreads over multiple memory cells through quantum spatial distribution and retrieves data from them in parallel [16, 17].

Recently, a different approach to implementing a universal quantum computation—one that motivates the present work—has been proposed, aiming to simplify the realization of non-trivial quantum gates compared to

circuit-based methods [18]. In this proposal, a single particle residing in a single square represents a three-qubit state. One qubit is represented by the coin state of the particle, and the other two qubits by its position—which of the four vertices the particle occupies. Furthermore, one can increase the number of qubits by two for each additional square placed in a nested structure [19] (in contrast to our model, only one particle is assigned a coin state).

This letter further extends the versatility of the quantum walk to quantum error correction by proposing a novel error-correcting scheme exploiting the quantum spatial distribution on nested squares. Because a single particle in a square can represent a three-qubit state via its coin and position states, Shor's nine-qubit error-correcting code can be implemented using only three particles, each allocated on a distinct square. Notably, encoding, error correction, and arbitrary operations on the encoded information are all accomplished using interactions only between nearest-neighbor particles, which is a capability enabled by the gauge symmetry [20–24].

*Multi-particle quantum walk on nested squares*— We begin by formulating the multi-particle quantum walk on nested squares. All particles have both coin and position states, spanned respectively by  $\{|0\rangle_c, |1\rangle_c\} \subset \mathbb{C}^2$

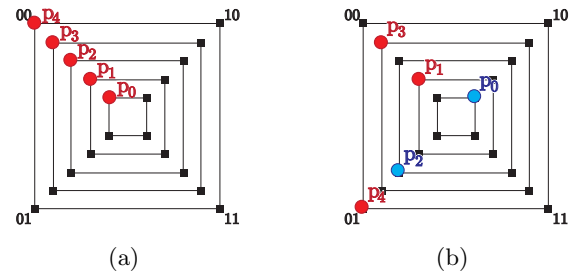


FIG. 1. The three-particle system  $\{p_0, p_2, p_4\}$  with ancillary particles  $\{p_1, p_3\}$  for syndrome measurement. The state in (a) is written as  $(|0\rangle_c|00\rangle_{xy})_{p_4} (|0\rangle_c|00\rangle_{xy})_{p_2} (|0\rangle_c|00\rangle_{xy})_{p_0}$ , and in (b) as  $(|1\rangle_c|10\rangle_{xy})_{p_4} (|1\rangle_c|10\rangle_{xy})_{p_2} (|1\rangle_c|01\rangle_{xy})_{p_0}$ , where red represents the state  $|0\rangle_c$  while blue represents  $|1\rangle_c$ .

\* asaka@rs.tus.ac.jp

† 1223550@ed.tus.ac.jp

and  $\{|00\rangle_{xy}, |10\rangle_{xy}, |11\rangle_{xy}, |01\rangle_{xy}\} \subset \mathbb{C}^4$  with the  $xy$ -coordinate rule.

We assume five particles/squares to demonstrate the implementation of Shor's nine-qubit code. The particles are labeled  $p_0$ - $p_4$  from the innermost to the outermost square (Fig. 1). The set of particles  $\{p_0, p_2, p_4\}$  will be used to host the redundantly encoded single-qubit information that is protected by our error-correcting scheme, whereas  $\{p_1, p_3\}$  serves as ancillary qubits for error detection.

In our quantum walk, all particles evolve through the iterative application of coin-flipping ( $\mathcal{C}$ ) and position-shifting ( $\mathcal{S}$ ), which are standard operations in conventional quantum walks, together with neighboring in-

teractions ( $\mathcal{N}$ ) introduced to account for multi-particle dynamics. First, each particle updates its coin state through the coin-flipping operation, depending on the vertex this particle occupies. The subsequent position-shifting either keeps the particle stationary or moves it to the next vertex in a clockwise direction on the same square, depending on whether the coin state is  $|0\rangle_c$  or  $|1\rangle_c$ . Finally, each pair of particles on adjacent squares acquires a phase factor of  $-1$  through neighboring interactions if they have the same coin state and occupy nearest-neighbor vertices, i.e., vertices on adjacent squares that share the same  $x$  and  $y$  coordinates. Explicitly, all particles evolve under the action of the following three operators:

$$\begin{aligned} \mathcal{C} &:= \prod_{i=0}^4 \left( \sum_{xy=00}^{11} U_c^{(i;xy)} \otimes |xy\rangle\langle xy|_{xy} \right)_{p_i}, \quad \mathcal{S} := \prod_{i=0}^4 \left( |0\rangle\langle 0|_c \otimes I_{xy} + |1\rangle\langle 1|_c \otimes R_{xy} \right)_{p_i}, \\ \mathcal{N} &:= \prod_{i=0}^3 \left( (I_c \otimes I_{xy})^{\otimes 2} - 2 \sum_{c=0}^1 \sum_{xy=00}^{11} (|c\rangle\langle c|_c \otimes |xy\rangle\langle xy|_{xy})^{\otimes 2} \right)_{p_i, p_{i+1}}. \end{aligned} \quad (1)$$

These operators are applied in the sequence  $\mathcal{C} \rightarrow \mathcal{S} \rightarrow \mathcal{N} \rightarrow \mathcal{C} \rightarrow \dots$ . The right-side subscript " $p_i$ " (resp. " $p_i, p_{i+1}$ ") indicates that the operator inside the parentheses acts nontrivially on the particle  $p_i$  (resp. the particles  $p_i$  and  $p_{i+1}$ ). The component  $U_c^{(i;xy)} \in \text{End}(\mathbb{C}^2)$  thus represents a unitary operator acting on the coin state of the corresponding particle. This may be a specific operator, such as the identity  $I_c := |0\rangle\langle 0|_c + |1\rangle\langle 1|_c$ , Pauli  $X$  operator  $X_c := |1\rangle\langle 0|_c + |0\rangle\langle 1|_c$ , Pauli  $Z$  operator  $Z_c := |0\rangle\langle 0|_c - |1\rangle\langle 1|_c$ , or Hadamard operator  $H_c := (Z_c + X_c)/\sqrt{2}$ . Additionally, the operator  $I_{xy} \in \text{End}(\mathbb{C}^4)$  is the identity for the position state, meaning that it keeps the particle stationary. The operator  $R_{xy}$  is defined as  $R_{xy} := |10\rangle\langle 00|_{xy} + |11\rangle\langle 10|_{xy} + |01\rangle\langle 11|_{xy} + |00\rangle\langle 01|_{xy} \in \text{End}(\mathbb{C}^4)$ , which moves the particle in a clockwise direction.

*Error model*— We naturally introduce two types of unintended unitary operations: a coin-flipping error  $E_C$  and a position-shifting error  $E_S$ . They are defined as

$$E_C = \sum_{x,y \in \{0,1\}} E_c^{(xy)} \otimes |xy\rangle\langle xy|_{xy}, \quad (2)$$

$$E_S = \sum_{j \in \{0,1\}} |c\rangle\langle c|_c \otimes (\alpha_j I_{xy} + \beta_j R_{xy} + \gamma_j R_{xy}^\top) \quad (3)$$

where  $E_c^{(xy)} \in \text{End}(\mathbb{C}^2)$ . The coefficients  $\alpha_j, \beta_j, \gamma_j \in \mathbb{C}$  ( $j = 0, 1$ ) are chosen such that  $E_S$  is unitary.

Throughout this letter, we assume that these two types of errors do not occur simultaneously, as they originate from different physical sources. Specifically, the error  $E_C$  is attributed to a malfunction in the coin-flipping operation  $\mathcal{C}$  or disturbances from external noise. In contrast,

$E_S$  can be regarded as an unintended position shift that either advances one step ahead or lags one step behind the intended position, which may depend on the coin state or occur independently of it.

Here, we do not consider an error that unintentionally moves a particle from one specific vertex to another, since it is non-unitary despite being intuitive. However, a similar effect arises within the above unitary framework if  $E_C$  occurs just before the intended shift operation  $\mathcal{S}$ : first,  $E_C$  flips the coin state from  $|0\rangle_c$  to  $|1\rangle_c$  for a particle that was meant to remain stationary at a vertex and subsequently, the scheduled  $\mathcal{S}$  unintentionally moves this particle to the next vertex.

*Quantum walk error correction*— The following explanation demonstrates that iterations of  $\mathcal{C}$ ,  $\mathcal{S}$ , and  $\mathcal{N}$  correct either the error  $E_C$  or  $E_S$  in at most one particle within the system  $\{p_0, p_2, p_4\}$ . During this process, the components of  $\mathcal{C}$  are updated sequentially and the ancillary set  $\{p_1, p_3\}$  is measured periodically. To simplify the explanation, we assume that  $E_S$  or  $E_C$  can occur between completing one cycle and starting the next cycle of the correction. Here, one cycle consists of aggregating the eigenvalues of the six stabilizer generators  $s_0$ – $s_5$  in Table I by measuring  $\{p_1, p_3\}$ .

Note that the states of  $\{p_0, p_2, p_4\}$  that the following scheme can protect against either  $E_C$  [Eq. (2)] or  $E_S$  [Eq. (3)] are limited to only the  $s_0$ – $s_5$  simultaneous eigenstates. However, this is sufficient for the purpose of quantum error correction. Namely, we can redundantly encode single-qubit information into this system as the simultaneous eigenstate (see the next section).

Measuring the  $s_0$ – $s_5$  eigenvalues—known as *syndrome measurement*—achieves twofold objectives. First, the

TABLE I. Stabilizer generators  $s_i$  ( $0 \leq i \leq 5$ ), gauge transformations ( $g_i^Z, g_i^X$ ) ( $0 \leq i \leq 1$ ), and the logical Z and X operators ( $\bar{X}, \bar{Y}$ ). The symbols Z and X represent the Pauli Z and X operators, respectively, and the subscripts c, x, or y indicate the state of the corresponding particle on which the operator acts.

$s_0 = (I_c \ I_x \ I_y)_{p_4} \otimes (Z_c \ Z_x \ I_y)_{p_2} \otimes (Z_c \ Z_x \ I_y)_{p_0},$
$s_1 = (I_c \ I_x \ I_y)_{p_4} \otimes (Z_c \ I_x \ Z_y)_{p_2} \otimes (Z_c \ I_x \ Z_y)_{p_0},$
$s_2 = (Z_c \ Z_x \ I_y)_{p_4} \otimes (Z_c \ Z_x \ I_y)_{p_2} \otimes (I_c \ I_x \ I_y)_{p_0},$
$s_3 = (Z_c \ I_x \ Z_y)_{p_4} \otimes (Z_c \ I_x \ Z_y)_{p_2} \otimes (I_c \ I_x \ I_y)_{p_0},$
$s_4 = (I_c \ I_x \ I_y)_{p_4} \otimes (X_c \ X_x \ X_y)_{p_2} \otimes (X_c \ X_x \ X_y)_{p_0},$
$s_5 = (X_c \ X_x \ X_y)_{p_4} \otimes (X_c \ X_x \ X_y)_{p_2} \otimes (I_c \ I_x \ I_y)_{p_0},$
$g_0^Z = (Z_c \ Z_x \ I_y)_{p_4} \otimes (I_c \ I_x \ I_y)_{p_2} \otimes (I_c \ I_x \ I_y)_{p_0}$
$g_1^Z = (Z_c \ I_x \ Z_y)_{p_4} \otimes (I_c \ I_x \ I_y)_{p_2} \otimes (I_c \ I_x \ I_y)_{p_0}$
$g_0^X = (X_c \ I_x \ X_y)_{p_4} \otimes (X_c \ I_x \ X_y)_{p_2} \otimes (X_c \ I_x \ X_y)_{p_0}$
$g_1^X = (X_c \ X_x \ I_y)_{p_4} \otimes (X_c \ X_x \ I_y)_{p_2} \otimes (X_c \ X_x \ I_y)_{p_0}$
$\bar{Z} = (Z_c \ Z_x \ Z_y)_{p_4} \otimes (Z_c \ Z_x \ Z_y)_{p_2} \otimes (Z_c \ Z_x \ Z_y)_{p_0}$
$\bar{X} = (X_c \ X_x \ X_y)_{p_4} \otimes (I_c \ I_x \ I_y)_{p_2} \otimes (I_c \ I_x \ I_y)_{p_0}$

measurement projects  $E_C$  or  $E_S$  in the particle  $p_0$ ,  $p_2$ , or  $p_4$  into bit- and phase-flip errors in the same particle. Second, we identify the projected errors based on how the eigenvalues have changed, as shown in Table II. The underlying mechanism is that both  $E_C$  and  $E_S$  are linear combinations of products of bit- and phase-flip errors, each product mapping the state of  $\{p_0, p_2, p_4\}$  into a different  $s_0$ - $s_5$  simultaneous eigenspace.

Here, an error that is part of the linear combination of  $E_C$  or  $E_S$  but not listed in Table II can be regarded as equivalent to one of the errors in this table via the gauge transformations and stabilizer generators in Table I. For example, because  $(I_c Z_x I_y)_{p_2} = g_0^Z s_2 (Z_c I_x I_y)_{p_2}$ , the error  $(I_c Z_x I_y)_{p_2}$  in  $E_S$  is treated as  $(Z_c I_x I_y)_{p_2}$  under the error correction. Namely, both errors result in the same syndrome pattern and have an equivalent effect on the system  $\{p_0, p_2, p_4\}$  where single-qubit information is encoded. We may refer to such equivalences as *gauge symmetry*, following the terminology in [20], and we will explain the reason for this gauge symmetry in the next section.

In the first step of the syndrome measurement, we determine the  $s_0$  and  $s_2$  eigenvalues. Initially, we allocate both ancillary particles  $p_1$  and  $p_3$  at the vertices labeled 00. Additionally, we set the components of  $\mathcal{C}$  as  $U_c^{(i;xy)} = X_c$  ( $i = 1, 3$ ,  $xy = 10, 11$ ), with the others as identities. Subsequently, we repeat  $\mathcal{C} \rightarrow \mathcal{S} \rightarrow \mathcal{N}$  over six times, with Hadamard operations applied to the coins at both the beginning and the end of the process to record the  $s_0$  and  $s_2$  eigenvalues into the coin states of  $p_1$  and  $p_3$ , respectively, as  $|0\rangle_c$  for +1 and  $|1\rangle_c$  for -1. This procedure is written as

$$(H_c)_{p_1} (H_c)_{p_3} (\mathcal{N} \mathcal{S} \mathcal{C})^6 (H_c)_{p_1} (H_c)_{p_3}, \quad (4)$$

with the identities omitted. Finally, we obtain  $m_0$  and  $m_2$  in Table II by measuring the coin states of  $\{p_1, p_3\}$ ,

TABLE II. The correspondence between the measured stabilizer syndrome and the operator mapped from a nontrivial unitary error on particle  $p_0$ ,  $p_2$ , or  $p_4$  by the syndrome measurement. The symbol  $m_i \in \{0, 1\}$  ( $0 \leq i \leq 5$ ) represents whether the measured eigenvalue of the stabilizer generator  $s_i$  has not flipped ( $m_i = 0$ ) or has flipped ( $m_i = 1$ ) from the previous cycle.

$m_5$	$m_4$	Phase flip	$m_3$	$m_2$	$m_1$	$m_0$	Bit flip
0	0	None	0	0	0	0	None
0	1	$(Z_c \ I_x \ I_y)_{p_0}$	0	0	0	1	$(I_c \ X_x \ I_y)_{p_0}$
1	0	$(Z_c \ I_x \ I_y)_{p_4}$	0	0	1	0	$(I_c \ I_x \ X_y)_{p_0}$
1	1	$(Z_c \ I_x \ I_y)_{p_2}$	0	0	1	1	$(X_c \ I_x \ I_y)_{p_0}$

$m_3$	$m_2$	$m_1$	$m_0$	Bit flip	$m_3$	$m_2$	$m_1$	$m_0$	Bit flip
0	1	0	0	$(I_c \ X_x \ I_y)_{p_4}$	0	1	0	1	$(I_c \ X_x \ I_y)_{p_2}$
1	0	0	0	$(I_c \ I_x \ X_y)_{p_4}$	1	0	1	0	$(I_c \ I_x \ X_y)_{p_2}$
1	1	0	0	$(X_c \ I_x \ I_y)_{p_4}$	1	1	1	1	$(X_c \ I_x \ I_y)_{p_2}$

both returned to vertex 00

The second step determines the  $s_1$  and  $s_3$  eigenvalues. Here, the particles  $\{p_0, p_2, p_4\}$  are initially shifted by two from their original states just before the previous step for  $s_0$  and  $s_2$  begins. For example, a particle originally at the vertex labeled 00 with  $|1\rangle_c$  is now at the vertex labeled 11. From this condition, the procedure for collecting the eigenvalues follows the same flow as Eq. (4), but the components of  $\mathcal{C}$  are set as  $U_c^{(i;xy)} = X_c$  ( $i = 1, 3$ ,  $xy = 11, 01$ ).

The final step is determining the remaining  $s_4$  and  $s_5$  eigenvalues. The shifts by two of the particles  $p_0$ ,  $p_2$ , and  $p_4$  are resolved through the previous step, and they have returned to their original positions. As a preparation, we need to transform the  $X_c X_x X_y$  eigenstates of  $\{p_0, p_2, p_4\}$  into the  $Z_c Z_x Z_y$  eigenstates with same eigenvalues. Such a transform can be achieved through the eight iterations  $(\mathcal{S} \mathcal{C})^8$ , where neighboring interactions must be prevented to avoid unintended phase shift of  $-1$ , i.e., influences from the ancillary particles  $p_1$  and  $p_3$ . Here, during the 3rd, 4th, and 5th steps in these iterations, the components of  $\mathcal{C}$  are set as follows, respectively:

$$H_c|00\rangle\langle 00|_{xy} + H'_c|10\rangle\langle 10|_{xy} + H_c|11\rangle\langle 11|_{xy} + H'_c|01\rangle\langle 01|_{xy}, \quad (5)$$

$$H_c|00\rangle\langle 00|_{xy} + H'_c|10\rangle\langle 10|_{xy} + H'_c|11\rangle\langle 11|_{xy} + H_c|01\rangle\langle 01|_{xy}, \quad (6)$$

$$H_c|00\rangle\langle 00|_{xy} + H_c|10\rangle\langle 10|_{xy} + H'_c|11\rangle\langle 11|_{xy} + H'_c|01\rangle\langle 01|_{xy} \quad (7)$$

for  $p_0$ ,  $p_2$ , and  $p_4$ , while in all other cases, they remain as identities. Here,  $H'_c := (X_c - Z_c)/\sqrt{2}$ . Subsequently, we measure the eigenvalues of these two generators through the same procedure as Eq. (4), but with components of  $\mathcal{C}$  set as  $U_c^{(i;xy)} = X_c$  ( $i = 1, 3$ ,  $xy = 10, 01$ ). Finally, we return the  $Z_c Z_x Z_y$  eigenstates of the particles to the  $X_c X_x X_y$  eigenstates with the same eigenvalues, through the same eight iterations  $(\mathcal{S} \mathcal{C})^8$  as described above.

In summary, we collect the syndrome pattern from  $m_0 - m_5$ , which represents how the  $s_0 - s_5$  eigenvalues change from the previous cycle, via 32 iterations of  $\mathcal{C}$ ,  $\mathcal{S}$ , and  $\mathcal{N}$ , along with periodic measurements of the ancillary set  $\{p_1, p_3\}$ . During these iterations, each particle loops up to six and a half times along the square vertices. We repeatedly perform this syndrome measurement and monitor the flipping errors accumulating in the system  $\{p_0, p_2, p_4\}$  via the syndrome patterns. Note that we need to swap the measurement order for  $(s_0, s_2)$  and  $(s_1, s_3)$  in each cycle of the syndrome measurement, because the shift by two, mentioned earlier, also occurs during the measurement for  $(s_4, s_5)$ .

Here, we do not need to correct emerging flipping errors after each cycle of syndrome measurement. Namely, the historical record of syndrome patterns always provides a way to correct the accumulated flipping errors, as these errors all commute with the syndrome measurements.

*Information encoding*— We now describe that iterations of  $\mathcal{C}$ ,  $\mathcal{S}$ , and  $\mathcal{N}$  can also redundantly encode single-qubit information into the system  $\{p_0, p_2, p_4\}$ . Because the encoded state is a simultaneous eigenstate of  $s_0 - s_5$  in Table I, the information gains resilience against the errors  $E_C$  [Eq. (2)] and  $E_S$  [Eq. (3)] under our previously discussed error-correcting scheme. Explicitly, we represent the encoded state as  $\alpha|0\rangle_L + \beta|1\rangle_L \in (\mathbb{C}^2)^{\otimes 9}$  ( $\alpha, \beta \in \mathbb{C}$ ), where  $|0\rangle_L$  and  $|1\rangle_L$  lie in the same simultaneous eigenspace and thus yield the same syndrome pattern.

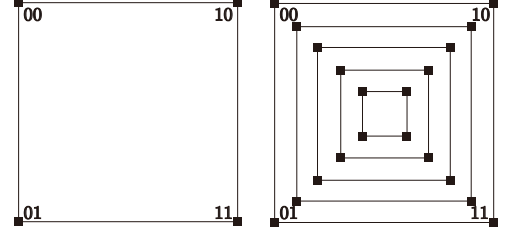
To understand the specific form of these two states  $|0\rangle_L$  and  $|1\rangle_L$ , it is important to consider that their simultaneous eigenspace consists of three virtual qubits [20] (this space naturally has the structure of  $(\mathbb{C}^2)^{\otimes 3}$ , because each of  $s_0 - s_5$  divides the nine-qubit Hilbert space equally into its  $+1$  and  $-1$  eigenstates). One is referred to as the virtual logical qubit, whose computational  $Z$ - and  $X$ -basis states are defined by the anticommuting pair of logical operators  $(\bar{Z}, \bar{X})$  in Table I. The remaining two are referred to as virtual gauge qubits, each of which has a pair of gauge transformations  $(g_i^X, g_i^Z)$  ( $i \in \{0, 1\}$ ) in the same table defining its computational basis states.

Notably, the two states  $|0\rangle_L$  and  $|1\rangle_L$  are distinguished by which computational  $Z$ -basis state the virtual logical qubit takes. Namely, they are  $+1$  and  $-1$  eigenstates of the logical operator  $\bar{Z}$ . These states are, of course, protected by our error-correcting scheme as they are also  $s_0 - s_5$  simultaneous eigenstates.

Meanwhile, two virtual gauge qubits do not carry useful information but reflect the presence of the gauge symmetry. Namely, they partly absorb a flipping error—a summand in  $E_C$  or  $E_S$ —that the syndrome measurement cannot detect, and then manifest it as a detectable error in Table II. For example, because the transformation  $g_0^Z$  acts only on one of the virtual gauge qubits, our error-correcting scheme can, as mentioned earlier, treat the error  $(I_c Z_x I_y)_{p_2}$  unlisted in this Table as equivalent to  $(Z_c I_x I_y)_{p_2}$  with  $g_0^Z$  seemingly absorbed. Here,  $g_0^Z$  does not change the syndrome pattern as it commutes all sta-

bilizer generators.

To encode information into the virtual logical qubit of the system  $\{p_0, p_2, p_4\}$ , we place an additional square to the left of the outermost square where the particle  $p_4$  exists:



Additionally, we set the external particle labeled  $p_{\text{ex}}$  with coin state  $|0\rangle_c$  at the vertex 00 of this extended square. This external particle exhibits the same evolution as other particles that follow the operator  $\mathcal{C}$ ,  $\mathcal{S}$ , and  $\mathcal{N}$ . Here, the interaction between the adjacent pair of particles  $p_{\text{ex}}$  and  $p_4$  occurs when  $p_{\text{ex}}$  is located at the vertex 00 (resp. 10) and  $p_4$  at the vertex 00 (resp. 01).

As a preliminary step for encoding, we initially prepare the logical state  $|0\rangle_L$  by measuring the eigenvalues of the six stabilizer generators  $s_0 - s_5$  and the logical operator  $\bar{Z}$ . From this point, the state  $|0\rangle_L$  is regarded as the obtained simultaneous eigenstate corresponding to the measured syndrome and the eigenvalue of  $\bar{Z}$  (if its eigenvalue of  $\bar{Z}$  is reversed, the state becomes  $|1\rangle_L$ ).

Subsequently, by a trivial procedure, we prepare single-qubit information in the coin state of  $p_{\text{ex}}$  located at the vertex 00, and then encode this information to the virtual logical qubit. This encoding is specifically achieved in three stages:

$$\{(\alpha|0\rangle_c + \beta|1\rangle_c)\}_{p_{\text{ex}}} |0\rangle_L \quad (8)$$

$$\xrightarrow{(i)} \alpha(|0\rangle_c)_{p_{\text{ex}}} |0\rangle_L + \beta(|1\rangle_c)_{p_{\text{ex}}} |1\rangle_L \quad (9)$$

$$\xrightarrow{(ii)} (|0\rangle_c)_{p_{\text{ex}}} (a|0\rangle_L + b|1\rangle_L)/\sqrt{2} + (|1\rangle_c)_{p_{\text{ex}}} (a|0\rangle_L - b|1\rangle_L)/\sqrt{2} \quad (10)$$

$$\xrightarrow{(iii)} (|c\rangle_c)_{p_{\text{ex}}} (a|0\rangle_L + b|1\rangle_L) \quad (c \in \{0, 1\}), \quad (11)$$

where we abbreviate  $(|c\rangle_c|00\rangle_{xy})_{p_{\text{ex}}}$  as  $(|c\rangle_c)_{p_{\text{ex}}}$  ( $c = 0, 1$ ). Here, (i) is applying the CNOT operation, with the coin state of  $p_{\text{ex}}$  as the control and the virtual logical qubit as the target, the implementation of which is described in the next paragraph (see Eq. (12)). Furthermore, (ii) is applying a Hadamard gate  $H_c$  to the particle  $p_{\text{ex}}$ , and (iii) consists of measuring the coin state of  $p_{\text{ex}}$  and applying the logical phase-flip  $\bar{Z}$  to the system  $\{p_0, p_2, p_4\}$  if  $|1\rangle_c$  is measured. Note that  $\bar{Z}$  can be simply performed by applying the  $Z_c$  to these three particles, given that  $\bigotimes_{i \in \{0, 2, 3\}} (Z_c I_x I_y)_{p_i} = (s_0 s_1 g_0^Z g_1^Z) \bar{Z}$ .

The above CNOT operation [(i) in Eq. (9)] results from 24 iterations:

$$\begin{aligned} & (\mathcal{SC})^8 (\mathcal{N} \mathcal{SC})^8 (\mathcal{SC})^8 \\ & \equiv (|0\rangle\langle 0|_c)_{p_{\text{ex}}} \otimes \bar{I} + (|1\rangle\langle 1|_c)_{p_{\text{ex}}} \otimes \bar{X}. \end{aligned} \quad (12)$$



where  $\bar{I}$  represents the identity for the whole system  $\{p_0, p_2, p_4\}$ . Here,  $(\mathcal{N}\mathcal{S}\mathcal{C})^8$  in the middle function as  $(|0\rangle\langle 0|_c)_{p_{\text{ex}}} \otimes (I_c I_y I_x)_{p_4} + (|1\rangle\langle 1|_c)_{p_{\text{ex}}} \otimes (Z_c Z_y Z_x)_{p_4}$  by the components of  $\mathcal{C}$  constantly being set as  $(X_c \otimes \sum_{xy} |xy\rangle\langle xy|_{xy})_{p_i}$  ( $i = 0, 2, 4$ ). Meanwhile, the first or last iterations  $(\mathcal{S}\mathcal{C})^8$  transform the  $(X_c X_x X_y)_{p_4}$  eigenstates into  $(Z_c Z_x Z_y)_{p_4}$ , or vice versa, by updating the components of  $\mathcal{C}$  for the particle  $p_4$ , as in the preparation procedure for the measurement of  $s_4$  and  $s_5$  eigenvalues (see Eqs.(5)-(7)). Then, given that the logical bit-flip is  $\bar{X} := (X_c X_x X_y)_{p_4}$ , we arrive at the equivalence in Eq. (12).

*Conclusion*— We have proposed a novel quantum error-correcting scheme via the multi-particle discrete-time quantum walk. Our scheme utilizes the quantum spatial distribution to implement the redundant encod-

ing, which allows Shor's nine-qubit code to be realized with only three particles. Furthermore, thanks to the gauge symmetry, the required interactions are only between nearest neighbors during encoding and error correction. We further show in the end matter that arbitrary operations can be implemented within the same unitary framework.

## ACKNOWLEDGMENTS

We would like to express our deepest gratitude to Kazumitsu Sakai for his constructive discussions and his thoughtful advice on this letter. This work was partially supported by Grant-in-Aid for JSPS Fellows No.23KJ1962 from the Japan Society for the Promotion of Science.

- 
- [1] Y. Aharonov, L. Davidovich, and N. Zagury, Quantum random walks, *Physical Review A* **48**, 1687 (1993).
  - [2] J. Kempe, Quantum random walks: an introductory overview, *Contemporary Physics* **44**, 307 (2003).
  - [3] N. Shenvi, J. Kempe, and K. B. Whaley, Quantum random-walk search algorithm, *Physical Review A* **67**, 052307 (2003).
  - [4] V. Potoček, A. Gábris, T. Kiss, and I. Jex, Optimized quantum random-walk search algorithms on the hypercube, *Physical Review A—Atomic, Molecular, and Optical Physics* **79**, 012325 (2009).
  - [5] B. Hein and G. Tanner, Quantum search algorithms on the hypercube, *Journal of Physics A: Mathematical and Theoretical* **42**, 085303 (2009).
  - [6] A. Ambainis, J. Kempe, and A. Rivosh, Coins make quantum walks faster, *arXiv preprint quant-ph/0402107* (2004).
  - [7] R. Portugal, *Coined Walks on Infinite Lattices. In: Quantum Walks and Search Algorithms*, Vol. 19 (Springer, 2013).
  - [8] M. Szegedy, Quantum speed-up of markov chain based algorithms, in *45th Annual IEEE symposium on foundations of computer science* (IEEE, 2004) pp. 32–41.
  - [9] M. L. Rhodes and T. G. Wong, Quantum walk search on the complete bipartite graph, *Physical Review A* **99**, 032301 (2019).
  - [10] F. Peng, M. Li, and X. Sun, Deterministic discrete-time quantum walk search on complete bipartite graphs, *Physical Review Research* **6**, 033042 (2024).
  - [11] S. D. Berry and J. B. Wang, Quantum-walk-based search and centrality, *Physical Review A—Atomic, Molecular, and Optical Physics* **82**, 042333 (2010).
  - [12] G. A. Bezerra, P. H. Lugão, and R. Portugal, Quantum-walk-based search algorithms with multiple marked vertices, *Physical Review A* **103**, 062202 (2021).
  - [13] K. Mukai and N. Hatano, Discrete-time quantum walk on complex networks for community detection, *Physical Review Research* **2**, 023378 (2020).
  - [14] N. B. Lovett, S. Cooper, M. Everitt, M. Trevers, and V. Kendon, Universal quantum computation using the discrete-time quantum walk, *Physical Review A* **81**, 042330 (2010).
  - [15] V. Giovannetti, S. Lloyd, and L. Maccone, Quantum random access memory, *Physical review letters* **100**, 160501 (2008).
  - [16] R. Asaka, K. Sakai, and R. Yahagi, Quantum random access memory via quantum walk, *Quantum Science and Technology* **6**, 035004 (2021).
  - [17] R. Asaka, K. Sakai, and R. Yahagi, Two-level quantum walkers on directed graphs. ii. application to quantum random access memory, *Physical Review A* **107**, 022416 (2023).
  - [18] S. Singh, P. Chawla, A. Sarkar, and C. Chandrashekar, Universal quantum computing using single-particle discrete-time quantum walk, *Scientific Reports* **11**, 11551 (2021).
  - [19] P. Chawla, S. Singh, A. Agarwal, S. Srinivasan, and C. Chandrashekar, Multi-qubit quantum computing using discrete-time quantum walks on closed graphs, *Scientific Reports* **13**, 12078 (2023).
  - [20] D. Poulin, Stabilizer formalism for operator quantum error correction, *Physical review letters* **95**, 230504 (2005).
  - [21] D. Kribs, R. Laflamme, and D. Poulin, Unified and generalized approach to quantum error correction, *Physical review letters* **94**, 180501 (2005).
  - [22] D. W. Kribs, R. Laflamme, D. Poulin, and M. Lesosky, Operator quantum error correction, *Quantum Information & Computation* **6**, 383 (2006).
  - [23] D. Bacon, Operator quantum error-correcting subsystems for self-correcting quantum memories, *Physical Review A—Atomic, Molecular, and Optical Physics* **73**, 012340 (2006).
  - [24] G. Dauphinais, D. W. Kribs, and M. Vasmer, Stabilizer formalism for operator algebra quantum error correction, *Quantum* **8**, 1261 (2024).
  - [25] C. M. Dawson and M. A. Nielsen, The solovay-kitaev algorithm, *arXiv preprint quant-ph/0505030* (2005).
  - [26] M. A. Nielsen and I. L. Chuang, *Quantum computation and quantum information* (Cambridge university press, 2010).
  - [27] D. Gottesman, Theory of fault-tolerant quantum computation, *Physical Review A* **57**, 127 (1998).

## End Matter

*Single-qubit logical operation*— One might need to update the encoded information by operating on the virtual logical qubit. Let us discuss implementations of the logical Hadamard gate ( $\bar{H}$ ), phase gate ( $\bar{S}$ ), and  $\pi/8$  gate ( $\bar{T}$ ), which are known to efficiently enable arbitrary updates on the single-qubit information [25, 26]. Specifically, we here explain that these implementations can also be performed through the operations  $\mathcal{C}$ ,  $\mathcal{S}$ , and  $\mathcal{N}$ .

The logical gates  $\bar{H}$  and  $\bar{S}$ , are implemented simply by applying the coin-flipping operator  $\mathcal{C}$  only once to all particles  $p_0$ ,  $p_2$ , and  $p_4$ . Here, all components of  $\mathcal{C}$ , i.e.,  $U_c^{(i;xy)}$  ( $i = 0, 2, 4$ ,  $x, y = 0, 1$ ), are set to either  $H_c$  or  $Z_c S_c$ , respectively, where  $S_c := e^{-i\frac{\pi}{4}Z_c}$ . Namely, we can explicitly define these two gates as

$$\bar{H} := \bigotimes_{i \in \{0, 2, 4\}} (H_c I_x I_y)_{p_i}, \quad (13)$$

$$\bar{S} := \bigotimes_{i \in \{0, 2, 4\}} ((Z_c S_c) \otimes I_x \otimes I_y)_{p_i}. \quad (14)$$

The validity of Eq. (13) follows from the fact that it satisfies the criteria for the logical Hadamard gate [26, 27]:

$$\bar{H} \bar{Z} \bar{H}^\dagger = g \bar{X}, \quad \bar{H} \bar{X} \bar{H}^\dagger = g \bar{Z}. \quad (15)$$

where  $g := (g_0^Z g_1^Z s_0 s_1)(g_0^X g_1^X s_4)$ . Note that to derive the above equations, we have used the following identities:

$$\bar{Z} = (g_0^Z g_1^Z s_0 s_1) [(Z_c I_x I_y)_{p_4} (Z_c I_x I_y)_{p_2} (Z_c I_x I_y)_{p_0}], \quad (16)$$

$$\bar{X} = (g_0^X g_1^X s_4) [(X_c I_x I_y)_{p_4} (X_c I_x I_y)_{p_2} (X_c I_x I_y)_{p_0}]. \quad (17)$$

Additionally, the definition in Eq. (14) similarly satisfies the criteria for the phase gate as

$$\bar{S} \bar{Z} \bar{S}^\dagger = g \bar{Z}, \quad \bar{S} \bar{X} \bar{S}^\dagger = g(i \bar{X} \bar{Z}). \quad (18)$$

Here, we can ignore the gauge transformations in Eqs. (15) and (18) when validating the criteria, provided that the virtual logical qubit is transformed appropriately and remains disentangled from any virtual gauge qubits.

Meanwhile, the logical gate  $\bar{T}$ , which is equivalent to  $e^{-i(\pi/8)\bar{Z}}$ , is implemented through the external particle  $p_{\text{ex}}$ , as in the process for the encoding [Eqs.(8)–(11)]. Specifically, through the following three stages, we introduce a relative phase factor of  $e^{i\pi/4}$  between  $|0\rangle_L$  and  $|1\rangle_L$  in the encoded information, which corresponds to the action of the logical  $\bar{T}$  gate:

$$(|0\rangle_c)_{p_{\text{ex}}} (\alpha|0\rangle_L + \beta|1\rangle_L) \quad (19)$$

$$\xrightarrow{(i)} \alpha(|0\rangle_c)_{p_{\text{ex}}} |0\rangle_L + \beta(|1\rangle_c)_{p_{\text{ex}}} |1\rangle_L \quad (20)$$

$$\xrightarrow{(ii)} \alpha(|0\rangle_c)_{p_{\text{ex}}} |0\rangle_L + e^{i\frac{\pi}{4}} \beta(|1\rangle_c)_{p_{\text{ex}}} |1\rangle_L \quad (21)$$

$$\xrightarrow{(iii)} (|0\rangle_c)_{p_{\text{ex}}} (\alpha|0\rangle_L + e^{i\frac{\pi}{4}} \beta|1\rangle_L). \quad (22)$$

Here, (i) and (iii) are applying CNOT operations, with the virtual logical qubit as the control and the coin state

of  $p_{\text{ex}}$  as the target, the implementation of which is described in the following paragraph. Meanwhile, (ii) is applying  $e^{i(\pi/8)Z_c}$  to the coin state of  $p_{\text{ex}}$  (Eq. (21) omits a global phase factor).

The CNOT operations, which appear in both Eq. (20) and Eq. (22), are also implemented by a procedure similar to that for the CNOT in Eq. (12), although it requires measuring an  $g$  eigenvalue of the system  $\{p_0, p_2, p_4\}$ . To achieve this concretely, we first perform the iterations in Eq. (12), with the entire sequence is enclosed by  $H_c$  and  $\bar{H}$ , which results in a CPhase-like operation as

$$\begin{aligned} & \left( (H_c)_{p_{\text{ex}}} \bar{H} \right) \left( (SC)^8 (\mathcal{N}SC)^8 (SC)^8 \right) \left( (H_c)_{p_{\text{ex}}} \bar{H} \right) \\ & \equiv \left( (H_c)_{p_{\text{ex}}} \bar{H} \right) \\ & \quad \left( (|0\rangle\langle 0|_c)_{p_{\text{ex}}} \otimes \bar{I} + (|1\rangle\langle 1|_c)_{p_{\text{ex}}} \otimes \bar{X} \right) \left( (H_c)_{p_{\text{ex}}} \bar{H} \right) \\ & = (|+\rangle\langle +|_c)_{p_{\text{ex}}} \otimes \bar{I} + (|-\rangle\langle -|_c)_{p_{\text{ex}}} \otimes g \bar{Z}, \end{aligned} \quad (23)$$

partly using Eq. (15), where  $|\pm\rangle_c := (|0\rangle_c \pm |1\rangle_c)/\sqrt{2}$ . Subsequently, the CNOT operation in Eq. (20) or (22) is completed by measuring the  $g$  eigenvalue  $+1$  or  $-1$  and applying  $(X_c)_{p_{\text{ex}}}$  if  $-1$  is obtained. This is because the operator in Eq. (23) is rewritten as

$$\begin{aligned} & \frac{(1+g)}{2} \left( (I_c)_{p_{\text{ex}}} \otimes |0\rangle\langle 0|_L + (X_c)_{p_{\text{ex}}} \otimes |1\rangle\langle 1|_L \right) \\ & + \frac{(1-g)}{2} \left( (X_c)_{p_{\text{ex}}} \otimes |0\rangle\langle 0|_L + (I_c)_{p_{\text{ex}}} \otimes |1\rangle\langle 1|_L \right), \end{aligned} \quad (24)$$

where  $(1 \pm g)/2$  acts as the projector for system  $\{p_0, p_2, p_4\}$  onto the  $\pm 1$  eigenstate of  $g$ .

We determine the  $g$  eigenvalue by taking the product of three outcomes: the eigenvalues of  $s_4$ ,  $(g_0^Z g_1^Z s_0 s_1)$ , and  $(g_0^X g_1^X)$ , where the eigenvalue of  $s_4$  has already been obtained in the previous syndrome measurement. The eigenvalue of  $(g_0^Z g_1^Z s_0 s_1) = (I_c Z_x Z_y)_{p_4} (I_c Z_x Z_y)_{p_2} (I_c Z_x Z_y)_{p_0}$  can be obtained through six iterations of  $\mathcal{N}SC$  with two additional position-shifting  $\mathcal{S}$ .

Concretely, we first apply an additional  $\mathcal{S}$ , which is a necessary preparation step to correctly record the eigenvalue of  $(I_c Z_x Z_y)_{p_i}$  ( $i = 0, 2, 4$ ) into the coin state of  $p_1$  or  $p_3$ . Subsequently, we iterate  $\mathcal{N}SC$  six times, with  $(H_c)_{p_3} (H_c)_{p_1}$  applied before and after, similar to Eq. (4). During these iterations, the components of  $\mathcal{C}$  are set as  $U_c^{(i;xy)} = X_c$  ( $i = 1, 3$ ,  $xy = 01, 10$ ). Then, we measure the coin states of  $p_3$  and  $p_1$ ; the product of the measurement outcomes yields the eigenvalue of  $(g_0^Z g_1^Z s_0 s_1)$ . Finally, applying an additional  $\mathcal{S}$  again restores the system  $\{p_0, p_2, p_4\}$  to its original state.

The eigenvalue of  $(g_0^X g_1^X) = (I_c X_x X_y)_{p_4} (I_c X_x X_y)_{p_2} (I_c X_x X_y)_{p_0}$  can also be obtained through the same procedure as that for  $(g_0^Z g_1^Z s_0 s_1)$ , although the entire procedure must be enclosed by eight iterations  $(SC)^8$  that transform  $X_c X_x X_y$  eigenstates into  $Z_c Z_x Z_y$  eigenstates and vice versa.